

61 NH₂CH₂COOH · AgNO₃

61A Pure compound

No. 61A-1 NH₂CH₂COOH · AgNO₃, Glycine silver nitrate

(*M* = 244.94)

1a	Ferroelectricity in $\text{NH}_2\text{CH}_2\text{COOH} \cdot \text{AgNO}_3$ was discovered by Pepinsky et al. in 1957.		57Pep	
b	phase	II	I	57Pep
	state	F	P	
	crystal system		monoclinic	
	space group		$\text{P2}_1/\text{a} - \text{C}_{2\text{h}}^5$	
	$\theta [^\circ\text{C}]$	–55		
	$\theta = -43^\circ\text{C}$ for $\text{ND}_2\text{CH}_2\text{COOD} \cdot \text{AgNO}_3$.			77Ges
	$P_s \parallel [010]$.			57Pep
	$T_{\text{melt}} = 145^\circ\text{C}$.			72Moh
	$\rho = 2.79 \cdot 10^3 \text{ kg m}^{-3}$, $\rho_x = 2.806 \cdot 10^3 \text{ kg m}^{-3}$.			72Moh
	Transparent, colorless but usually brown as a result of illumination by light.			64Mit
	Cleavage plane: (010).			69Tod
2a	Crystal growth: cooling and evaporation methods from aqueous solution.			57Pep
	Slow introduction of ethyl alcohol vapor into the saturated aqueous solution.			57Pep
	Crystal form: Fig. 61A-1-001.			
3a	Unit cell parameters: $a = 5.451 \text{ \AA}$, $b = 19.493 \text{ \AA}$, $c = 5.541 \text{ \AA}$, $\beta = 100.20(25)^\circ$ in phase I.			72Moh
b	$Z = 4$ in phase I.			72Moh
	Crystal structure: Table 61A-1-001, Table 61A-1-002, Table 61A-1-003, Table 61A-1-004, Table 61A-1-005; Fig. 61A-1-002, Fig. 61A-1-003, Fig. 61A-1-004, Fig. 61A-1-005, Fig. 61A-1-006.			
4	Lattice distortions: Fig. 61A-1-007, Fig. 61A-1-008.			
5a	Dielectric constants: Fig. 61A-1-009, Fig. 61A-1-010, Fig. 61A-1-011.			
	Effect of hydrostatic pressure on partially deuterated crystal: see			77Ges
	$\kappa_b = C/(T - \theta_p)$, $T > \theta_p$, $C = 446 \text{ K}$, $\theta_p = -55^\circ\text{C}$.			64Mit
	Curie-Weiss constant changes with hydrostatic pressure as $C = C_0(1 + \beta p)$,			77Ges
	$C_0 = 860(40) \text{ K}$, $\beta = -0.17(2) \cdot 10^{-8} \text{ Pa}^{-1}$ in the range $p < 1.8 \cdot 10^8 \text{ Pa}$.			
	Phase diagram in regard to p : Fig. 61A-1-012.			
	Phase diagram for partially deuterated crystal: see			77Ges
b	Nonlinear dielectric properties: $\xi = 5.2 \cdot 10^{14} \text{ V m}^5 \text{ C}^{-3}$.			64Mit
c	Spontaneous polarization and coercive field: Fig. 61A-1-013, 61A-1-014.			
7b	Electrostrictive constants: $\Delta a/a P_s^2 = Q_{12} \approx -18 \text{ C}^{-2} \text{ m}^4$, $\Delta b/b P_s^2 = Q_{22} \approx 36 \text{ C}^{-2} \text{ m}^4$, $\Delta c/c P_s^2 \approx 300 \text{ C}^{-2} \text{ m}^4$, $\Delta \beta/\beta P_s^2 \approx 220 \text{ C}^{-2} \text{ m}^4$ at -100°C .			64Mit
13a	NMR: Fig. 61A-1-015.			

Table 61A-1-001. $\text{NH}_2\text{CH}_2\text{COOH} \cdot \text{AgNO}_3$. Structure of phase I [72Moh]. Fractional coordinates.

	Fractional coordinates				Fractional coordinates		
Ag	<i>x</i>	0.1450(4)	O(5)	<i>x</i>	−0.095(4)		
	<i>y</i>	0.01631(10)		<i>y</i>	0.1360(10)		
	<i>z</i>	−0.1855(4)		<i>z</i>	−0.038(4)		
O(1)	<i>x</i>	0.166(3)	N(1)	<i>x</i>	0.689(4)		
	<i>y</i>	0.0430(9)		<i>y</i>	0.1589(11)		
	<i>z</i>	0.401(3)		<i>z</i>	0.403(5)		
O(2)	<i>x</i>	0.412(3)	N(2)	<i>x</i>	0.047(4)		
	<i>y</i>	0.0645(9)		<i>y</i>	0.1884(10)		
	<i>z</i>	0.126(3)		<i>z</i>	−0.030(4)		
O(3)	<i>x</i>	0.151(3)	C(1)	<i>x</i>	0.355(5)		
	<i>y</i>	0.2074(10)		<i>y</i>	0.0710(12)		
	<i>z</i>	0.180(4)		<i>z</i>	0.333(5)		
O(4)	<i>x</i>	0.103(5)	C(2)	<i>x</i>	0.516(5)		
	<i>y</i>	0.2124(13)		<i>y</i>	0.1166(15)		
	<i>z</i>	−0.222(5)		<i>z</i>	0.524(6)		

Table 61A-1-002. $\text{NH}_2\text{CH}_2\text{COOH} \cdot \text{AgNO}_3$. Structure of phase I [72Moh]. Temperature parameter B_{ij} is defined by Eq. (a) in Introduction.

Ag	B_{11}	0.0275(6)	O(3)	B_{11}	0.035(7)	N(1)	B_{11}	0.030(7)
	B_{22}	0.00293(4)		B_{22}	0.0030(5)		B_{22}	0.0021(6)
	B_{33}	0.0314(6)		B_{33}	0.049(8)		B_{33}	0.046(9)
	B_{12}	−0.0061(3)		B_{12}	0.004(3)		B_{12}	−0.003(3)
	B_{13}	0.0041(11)		B_{13}	−0.022(12)		B_{13}	−0.010(14)
	B_{23}	−0.0035(3)		B_{23}	−0.006(3)		B_{23}	0.005(4)
O(1)	B_{11}	0.029(6)	O(4)	B_{11}	0.043(11)	N(2)	B_{11}	0.024(7)
	B_{22}	0.0032(5)		B_{22}	0.0053(9)		B_{22}	0.0020(5)
	B_{33}	0.032(7)		B_{33}	0.052(10)		B_{33}	0.052(10)
	B_{12}	−0.003(3)		B_{12}	−0.002(4)		B_{12}	0.001(3)
	B_{13}	−0.006(11)		B_{13}	−0.001(18)		B_{13}	−0.005(15)
	B_{23}	−0.004(3)		B_{23}	0.002(5)		B_{23}	−0.002(3)
O(2)	B_{11}	0.021(5)	O(5)	B_{11}	0.040(8)	C(1)	B_{11}	0.036(9)
	B_{22}	0.0027(5)		B_{22}	0.0021(5)		B_{22}	0.0013(5)
	B_{33}	0.032(6)		B_{33}	0.054(9)		B_{33}	0.033(10)
	B_{12}	−0.001(3)		B_{12}	−0.003(4)		B_{12}	−0.004(3)
	B_{13}	−0.004(9)		B_{13}	−0.018(15)		B_{13}	−0.036(14)
	B_{23}	−0.003(3)		B_{23}	−0.003(4)		B_{23}	−0.001(4)
						C(2)	B_{11}	0.028(9)
							B_{22}	0.023(8)
							B_{33}	0.034(13)
							B_{12}	−0.007(4)
							B_{13}	−0.014(19)
							B_{23}	−0.006(5)

Table 61A-1-003. NH₂CH₂COOH · AgNO₃. Structure of phase I [72Moh]. Interatomic distances around Ag atoms.

	Distance [Å]
Ag–O (1) (–x, –y, –z)	2.22(2)
Ag–O (2)	2.25(2)
Ag–O (1) (x, y, z – 1)	2.37(2)
Ag–O (2) (–x + 1, –y, –z)	2.85(2)
Ag–O (5)	2.86(2)
Ag–Ag (–x, –y, –z)	2.877(6)

Table 61A-1-004. NH₂CH₂COOH · AgNO₃. Structure of phase I [72Moh]. Interatomic angles around Ag atoms.

	Angle [deg]
O(1)(–x, –y, –z)–Ag–O(2)	163.1(7)
O(5)–Ag–O(2)(–x + 1, –y, –z)	146.7(5)
O(1)(x, y, z – 1)–Ag–Ag(–x, –y, –z)	149.9(4)
O(1)(–x, –y, –z)–Ag–O(5)	103.5(6)
O(5)–Ag–O(2)	73.0(6)
O(2)–Ag–O(2)(–x + 1, –y, –z)	73.9(6)
O(2)(–x + 1, –y, –z)–Ag–O(1)(–x, –y, –z)	109.0(6)
O(1)(x, y, z – 1)–Ag–O(5)	101.5(6)
O(5)–Ag–Ag(–x, –y, –z)	68.9(4)
Ag(–x, –y, –z)–Ag–O(2)(–x + 1, –y, –z)	110.9(4)
O(2)(–x + 1, –y, –z)–Ag–O(1)(x, y, z – 1)	92.8(5)
O(1)(–x, –y, –z)–Ag–O(1)(x, y, z – 1)	76.0(7)
O(1)(x, y, z – 1)–Ag–O(2)	120.9(6)
O(2)–Ag–Ag(–x, –y, –z)	84.7(4)
Ag(–x, –y, –z)–Ag–O(1)(–x, –y, –z)	79.1(5)
C(1)–O(2)–Ag	120.8(15)
O(1)–C(1)–O(2)	124.9(23)
Ag(–x, –y, –z)–O(1)–C(1)	130.0(17)

Table 61A-1-005. NH₂CH₂COOH · AgNO₃. Structure of phase I [72Moh]. Interatomic distances and angles in NO₃ group.

	Distance [Å]		Angle [deg]
N(2)–O(3)	1.26(3)	O(3)–N(2)–O(4)	123(2)
N(2)–O(4)	1.25(4)	O(3)–N(2)–O(5)	116(2)
N(2)–O(5)	1.28(3)	O(4)–N(2)–O(5)	120(2)

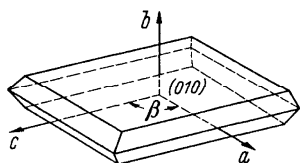


Fig. 61A-1-001. $\text{NH}_2\text{CH}_2\text{COOH} \cdot \text{AgNO}_3$. Crystal form [64Mit].

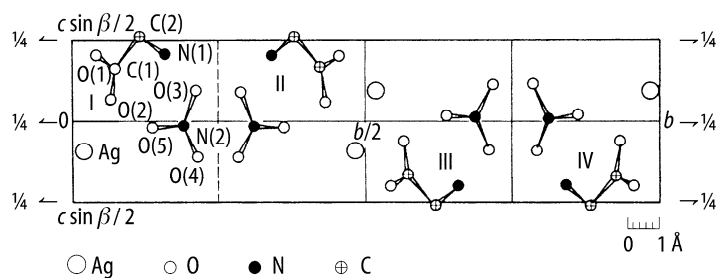


Fig. 61A-1-002. $\text{NH}_2\text{CH}_2\text{COOH} \cdot \text{AgNO}_3$. Structure of phase I [72Moh]. View along the a axis. The Roman numerals indicate the equivalent positions, and the relevant symmetry operations are as follows: I: x, y, z ; II: $1/2 + x, 1/2 - y, z$; III: $1/2 - x, 1/2 + y, -z$; IV: $-x, -y + 1, -z$.

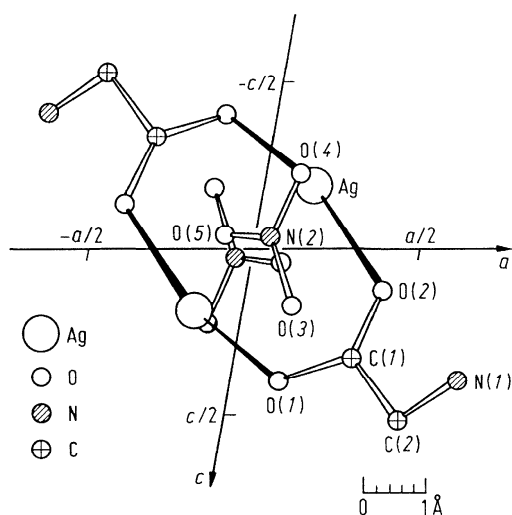


Fig. 61A-1-003. $\text{NH}_2\text{CH}_2\text{COOH} \cdot \text{AgNO}_3$. Structure of phase I [72Moh]. View along the b axis, showing the existence of glycine dimers bridged by silver atoms.

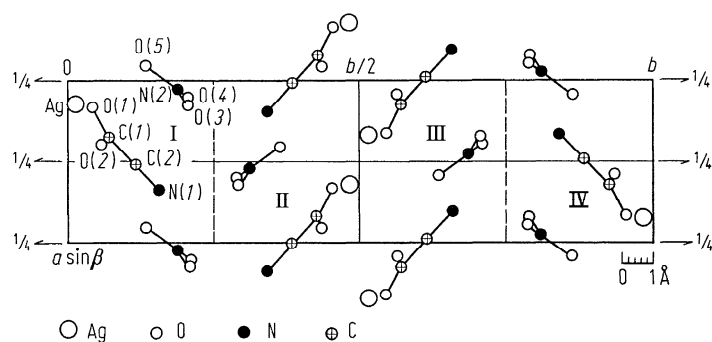


Fig. 61A-1-004. $\text{NH}_2\text{CH}_2\text{COOH} \cdot \text{AgNO}_3$. Structure of phase I [72Moh]. View along the c axis. See Fig. 61A-1-002 for Roman numerals.

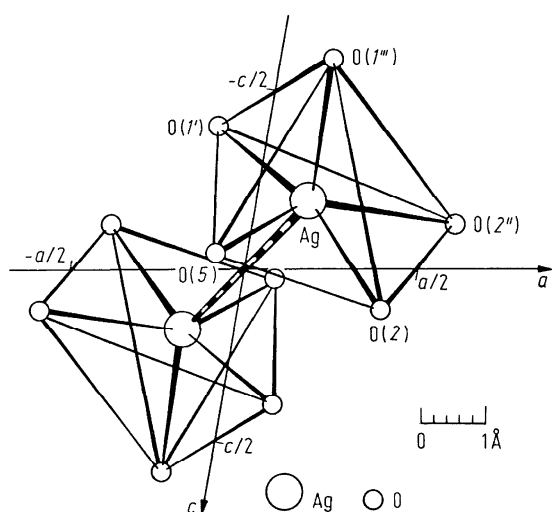


Fig. 61A-1-005. $\text{NH}_2\text{CH}_2\text{COOH} \cdot \text{AgNO}_3$. Structure of phase I [72Moh]. Surroundings of the inversion center at $(0, 0, 0)$. The Ag-Ag bond is represented by thick, partially shaded lines. The labelled atoms have the following coordinates: O(2), O(5), Ag: (x, y, z) ; O(1'): $(-x, -y, -z)$; O(2''): $(-x + 1, -y, -z)$; O(1''): $(x, y, z - 1)$.

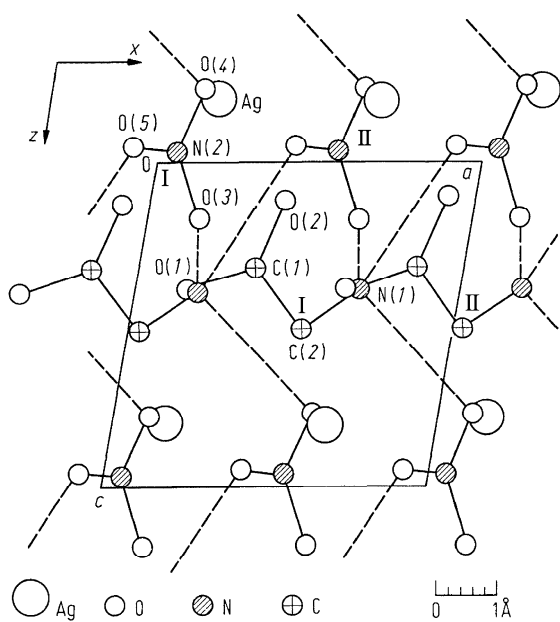


Fig. 61A-1-006. $\text{NH}_2\text{CH}_2\text{COOH} \cdot \text{AgNO}_3$. Structure of phase I [72Moh]. Hydrogen bondings (broken lines) viewed along the b axis. See Fig. 61A-1-002 for I and II.

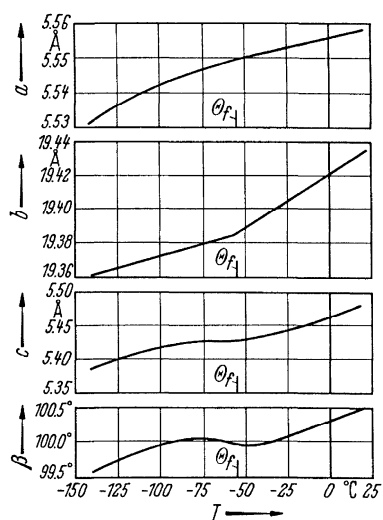


Fig. 61A-1-007. $\text{NH}_2\text{CH}_2\text{COOH} \cdot \text{AgNO}_3$. Lattice parameters vs. T [64Mit].

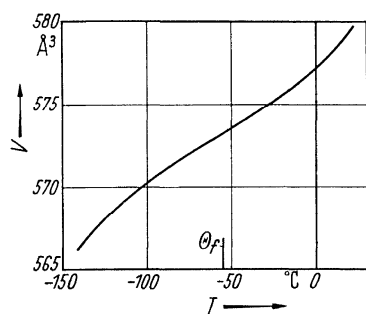


Fig. 61A-1-008. $\text{NH}_2\text{CH}_2\text{COOH} \cdot \text{AgNO}_3$. V vs. T [64Mit]. V : unit cell volume.

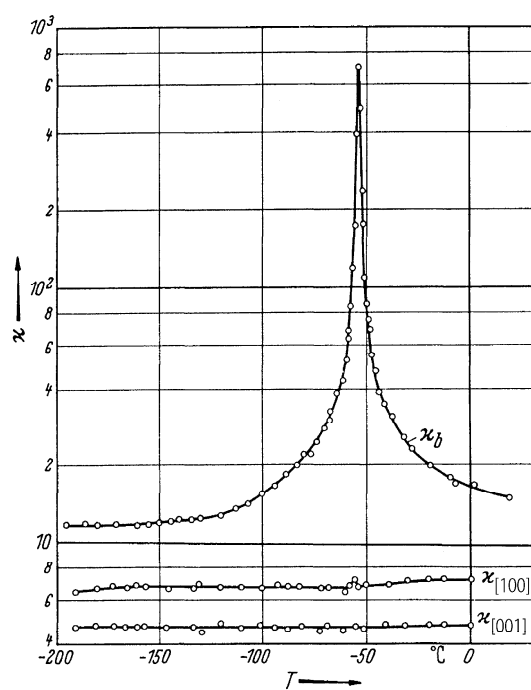


Fig. 61A-1-009. $\text{NH}_2\text{CH}_2\text{COOH} \cdot \text{AgNO}_3$. $\kappa_{[100]}$, κ_b , $\kappa_{[001]}$ vs. T [64Mit]. $f = 10$ kHz.

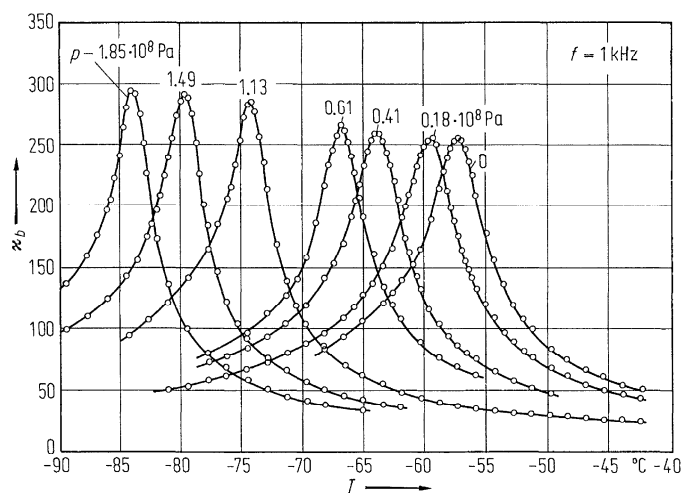


Fig. 61A-1-010. $\text{NH}_2\text{CH}_2\text{COOH} \cdot \text{AgNO}_3$. κ_b vs. T [77Ges]. Parameter: p .

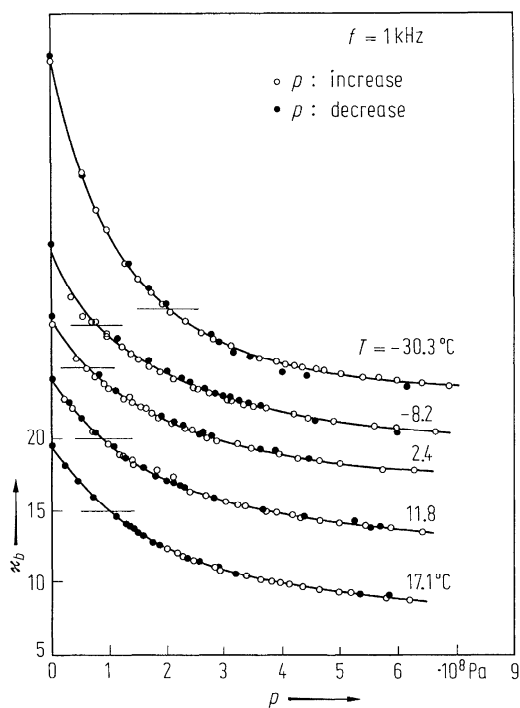


Fig. 61A-1-011. $\text{NH}_2\text{CH}_2\text{COOH} \cdot \text{AgNO}_3$. κ_b vs. p [77Ges]. Parameter: T . Thin horizontal lines show the level of $\kappa_b = 15$.

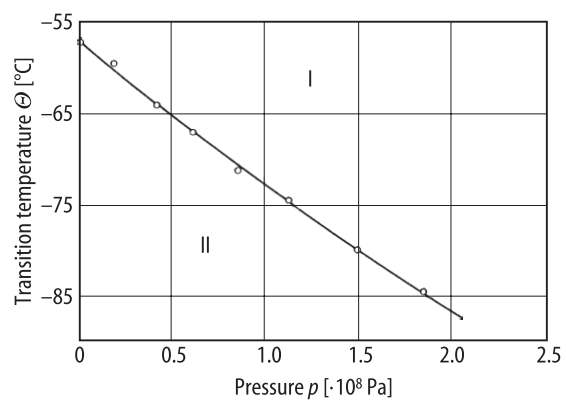


Fig. 61A-1-012. $\text{NH}_2\text{CH}_2\text{COOH} \cdot \text{AgNO}_3$. Θ vs. p [77Ges].

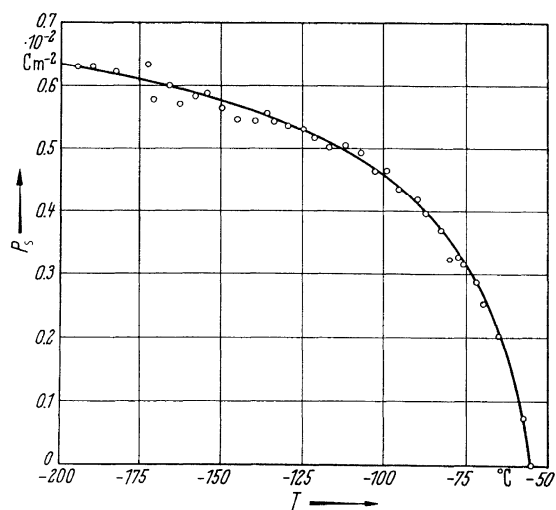


Fig. 61A-1-013. $\text{NH}_2\text{CH}_2\text{COOH} \cdot \text{AgNO}_3$. P_s vs. T [64Mit].

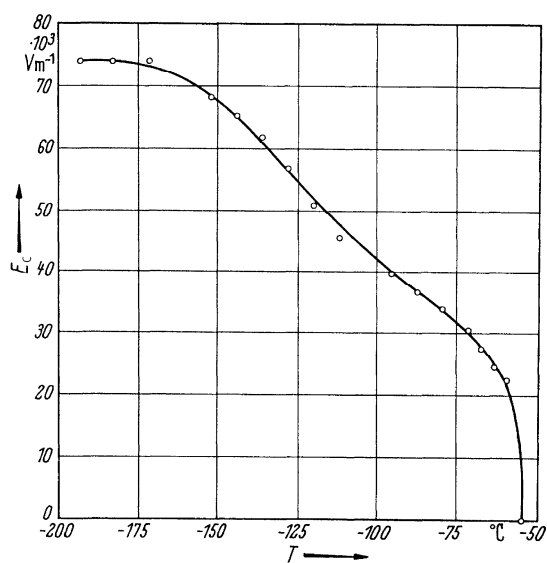


Fig. 61A-1-014. $\text{NH}_2\text{CH}_2\text{COOH} \cdot \text{AgNO}_3$. E_c vs. T [57Pep].

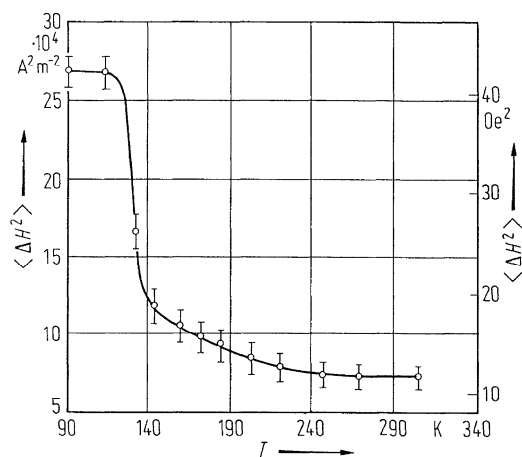


Fig. 61A-1-015. $\text{NH}_2\text{CH}_2\text{COOH} \cdot \text{AgNO}_3$. $\langle \Delta H^2 \rangle$ of proton vs. T [66Eas]. $\langle \Delta H^2 \rangle$: second moment of magnetic resonance curve.

References

- 57Pep Pepinsky, R., Okaya, Y., Eastman, D.P., Mitsui, T.: Phys. Rev. **107** (1957) 1538.
64Mit Mitani, S.: J. Phys. Soc. Jpn. **19** (1964) 481.
66Eas Easwaran, K.R.K.: J. Phys. Soc. Jpn. **21** (1966) 1614.
69Tod Todo, I., Tatsuzaki, I.: Phys. Status Solidi **32** (1969) 263.
72Moh Mohana Rao, J.K., Viswamitra, M.A.: Acta Crystallogr. Sect. B **28** (1972) 1484.
77Ges Gesi, K., Ozawa, K.: J. Phys. Soc. Jpn. **42** (1977) 923.